IEEE Access
Multidisciplinary | Rapid Review | Open Access Journal

Received July 29, 2021, accepted September 2, 2021, date of publication September 29, 2021, date of current version October 15, 2021.

Digital Object Identifier 10.1109/ACCESS.2021.3116144

Impact of Window Penetration Loss on Building Entry Loss From 3.5 to 24 GHz

YOUNG CHUL LEE[1], SOON-SOO OH[2], CHUL WOO BYEON[3], (Member, IEEE), KHAIRUNNISA AZIDING[1], AND BYUNG-LOK CHO[4]

[1]Division of Marine Mechatronics, Mokpo National Maritime University (MMU), Mokpo 58628, Republic of Korea
[2]Department of Electronic Engineering, Chosun University, Gwangju 61452, Republic of Korea
[3]Department of Electronic Engineering, Wonkwang University, Iksan 54538, Republic of Korea
[4]Division of Electrical and Electronics Engineering, Sunchon National University, Sunchon 57922, Republic of Korea

Corresponding author: Young Chul Lee (leeyc@mmu.ac.kr)

This work was supported by the Information & Communication Technology (ICT) R&D program of Ministry of Science and ICT (MSIT)/Institute for Information & Communication Technology Promotion (IITP) under Grant 2018-0-01439.

ABSTRACT We investigated the impact of window penetration loss (WinPL) on the frequency dependence of building entry loss (BEL) from 3.5 to 24 GHz. The WinPL characteristics of an ideal double-glazed glass and an actual double-glazed window were simulated and measured on-site, respectively, and both results showed almost the same oscillatory characteristics with respect to the frequency changes that occurred due to the impedance oscillation of the double glass-like multilayer dielectrics. Two BEL measurement scenarios were examined to analyze the frequency dependence of BEL in a traditional office building with double-glazed windows identical to those analyzed in the on-site WinPL measurements. The experiments included a complex propagation route (the first scenario) from the facade of the building to the corridors through windows and offices and a simple propagation route (the second scenario) through only windows lateral to the building. The two main findings are (i) BEL showed strong frequency-dependent behavior regardless of the propagation route and (ii) the WinPL characteristics of the outer double-glazed window were the main contributors to the frequency dependence of BEL.

INDEX TERMS Window penetration loss, building entry loss, outdoor-to-indoor propagation.

I. INTRODUCTION

Various investigations regarding outdoor-to-indoor (O2I) [1]–[7] and indoor-to-outdoor (I2O) [8] propagation have been attempted in previous studies on building entry loss (BEL), as penetration losses through building materials such as windows and walls directly affect the characteristics of BEL [3], [4], [7], [9]–[13]. Analyses based on these studies have improved understanding of propagation mechanisms and helped develop more sophisticated models.

In general, two methods are used to measure the penetration loss (PL) of a material: anechoic chamber measurements [4], [9], [11] and on-site measurements [3], [7], [12]. Usually, in a nonreflection chamber, the effects of reflections on measurements can be eliminated, allowing more accurate measurements. However, because building materials are made up of various inhomogeneous materials and are complex in structure, it is almost impossible to separate building materials from the building itself.

The associate editor coordinating the review of this manuscript and approving it for publication was Gokhan Apaydin.

Until recently, on-site measurements have been widely used for propagation research related to buildings; in these measurements, the effects of reflections should be considered [4]. In 2014, research results were reported regarding the impact of different illuminated areas and different radiation zones on the PL [3]. In this work, free-space loss measurements were performed at three different distances between a material under test (MUT) and a transmitter (or receiver). The results were mainly affected by distance, not by the ground reflections. In 2018, three on-site measurement methods, channel, far-field, and near-field measurements were compared to measure the PLs of office windows and walls [12]. The measurement results showed approximately the same PLs in the three cases. In addition, exciting results have reported on periodic window structures acting as band-cut filters due to internal reflections.

On-site measurements are usually time-consuming and costly. Therefore, simulations have been widely applied to research in this field because simulations can enhance the theoretical understanding of results and provide immediate inspiration for analyses [14]–[19]. In some measurement

results of the PLs of windows with double-glazed glass panes, it was reported that the PL did not increase linearly with increasing frequency; despite the different thicknesses and relative dielectric constants of the glass panes, similar oscillatory characteristics were observed, with high losses at 5 GHz and low losses at 10 GHz [7], [14], [18], [19]. These characteristics are due to the frequency dependence of an input impedance at the air-to-dielectrics interface [14] or to multiple internal reflective effects [12], [18].

Several simulations have been attempted using numerical models [14], Monte Carlo methods [19] or three-dimensional (3-D) tools [7] to analyze these phenomena, and the results can help researchers analyze nonlinear frequency dependence. However, it is difficult to accurately match actual measurement results with simulation results due to various factors, such as the inaccurate permittivity of glass or the angle of incidence of the radio waves.

The International Telecommunication Union (ITU) [20] published a standard prediction model of BEL in 2017. In this site-general model, two-building classes are considered: a traditional building and a thermally efficient building. The classification criterion involves whether modern and thermally efficient construction methods were used. In the case of a traditional building, the BEL model tends to increase linearly with increasing frequency. However, high BEL values were observed at specific low frequencies [7], [14].

The PL of building materials and BEL are useful for understanding building-related propagation characteristics. In particular, window penetration loss (WinPL) can be usefully applied to the frequency dependence analysis of O2I, I2O, and BEL, because most radio waves propagate through glass windows. However, until recently, few studies on propagation characteristics such as O2I, I2O, and BEL based on WinPL had been published.

In this paper, the frequency dependence of BEL is analyzed using simulated and measured WinPLs of double-glazed glass windows from 3.5 to 24 GHz. In section II, the oscillatory characteristics of WinPL for the studied double-glazed glass window are investigated using simulations and on-site measurement results of the window. Section III describes the BEL measurements, and their frequency dependence is analyzed in terms of the indoor terminal depth within the studied building. Finally, in section IV, we summarize the results.

II. WINDOW PENETRATION LOSS (WINPL) CHARACTERISTICS OF THE DOUBLE-GLAZED GLASS WINDOW

A. SIMULATION OF WINPL

The transmission properties of double-glazed glass were investigated using electromagnetic (EM) analysis software to analyze the characteristics of WinPLs of double-glazed glass windows [21]. Considering the computation time, a 3-D model of a double-glazed window with dimensions of 40 × 40 mm^2 was designed, as shown in Figure 1(a). The 3-D structure of the 24-mm double-glazed window involves

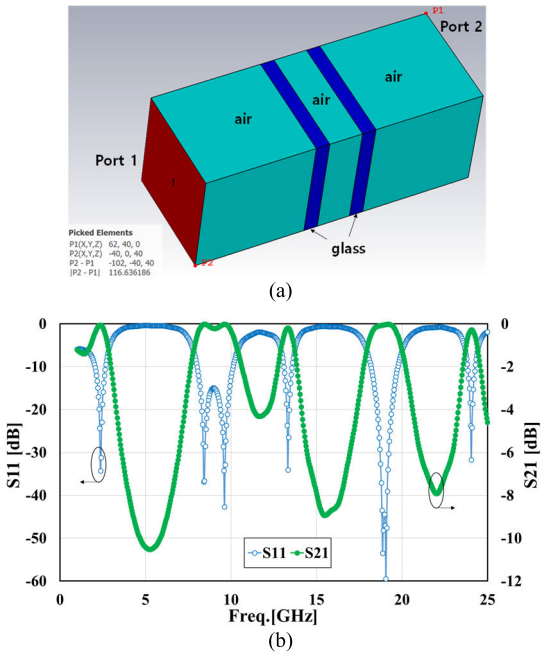

FIGURE 1. Simulation of the double-glazed glass: (a) 3-D model of the double-glazed glass, and (b) simulated insertion (S21) and return loss (S11) results.

two 6-mm-thick glass panes separated by a 12-mm air gap. The space between the glass and simulation port is filled with air. The distance between the two ports is 102 mm. A boundary condition for the bottom and top surfaces of the 3-D model is the perfect electric surface, and both side surfaces are assigned as the perfect magnetic surface. Therefore, transverse electromagnetic mode (TEM) propagation is possible inside the 3-D model, and its area is independent of the wavelength. The permittivity of the glass is 6.7 [18]. Figure 1 (b) presents the simulated insertion (S21) and return (S11) loss results. Very high insertion losses are observed at approximately 5.2, 11.7, 15.5, and 22 GHz. It can also be seen that the reflections (S11) are severe at these frequencies.

In contrast, low insertion losses and low reflection characteristics were observed at 2.4, 8.4, 9.6, 13.0, 18.9, 19.0, and 24.0 GHz. Incident radio waves passed through the two sheets of glass without reflection at these frequencies. In addition, 8.4–9.6 GHz and 18.9–19.0 GHz, respectively, exhibit band-like frequency characteristics. Double-glazed glass can behave in the same way as a multilayer dielectric sheet, and the transmission characteristics of double-glazed glass follow the ordinary transmission line theory. Therefore, the transmission characteristics of double-glazed glass mainly depend on the impedance change at a specific frequency. The insertion loss (S21) can be referred to as WinPL.

Figure 2 shows the electric-field distribution in the 3-D model of the studied double-glazed glass at frequencies that represent high and low insertion losses. It does not change in the direction perpendicular to the direction of propagation. Most of the electric fields are reflected from the double-glazed glass at 5.2, 11.7, 15.5, and 22 GHz, where high losses

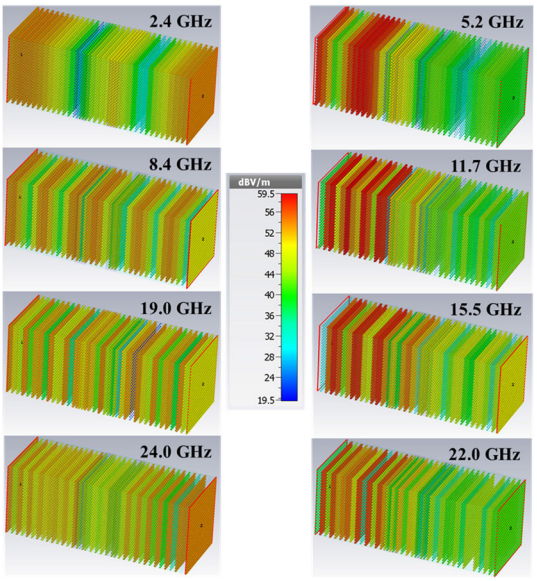

FIGURE 2. Electric field distribution at frequencies that represent high and low insertion losses [a phase: 200 degrees].

occur, although some weak fields are applied at port 2 for 15.5 GHz because of different phase velocity. Conversely, at frequencies such as 2.4, 8.4, 19.0, and 24 GHz, representing low S21 values, most of the waves propagate well through the glass.

In general, it is expected that WinPL of the double-glazed window will be affected by the construction of the glass and by its relative dielectric constant, as these are major parameters affecting changes in the impedance of a glass window. WinPL was calculated as a function of the glass construction and its permittivity. In this simulation, four commercially available double-glazed glass window structures were applied: 16-, 18-, 22-, and 24-mm double-glazed glass. In the case of the 16-mm glass, a 4-mm-thick intermediate air gap exists between two 6-mm-thick glass layers; this construction is denoted as 6–4–6 (glass-gap-glass). The structures of the 18-, 22-, and 24-mm glass windows are 6–6–6, 6–10–6, and 6–12–6, respectively. The relative dielectric constant of all the glass structures was 6.7 [18]. In the case of the 24-mm glass, WinPL was calculated by changing the permittivity of the glass to 6.0, 6.7, and 7.0 [18]. The simulated results are denoted in Figure 3. The frequency characteristics of WinPL are sensitively affected by glass construction, as shown in Figure 3 (a). The frequency characteristics of WinPL do not change significantly according to changes in the permittivity of glass, but these changes are expected to be significant at 20 GHz or higher, as shown in Figure 3 (b). In previously published research results [14], [18], [19], despite different glass permittivities and structures, high losses at approximately 5 GHz and low losses at approximately 10 GHz were reported; these results are consistent with our research results.

From the results of the WinPL simulation, it can be concluded that WinPL does not increase linearly due to a change in the impedance of the window as the frequency increases,

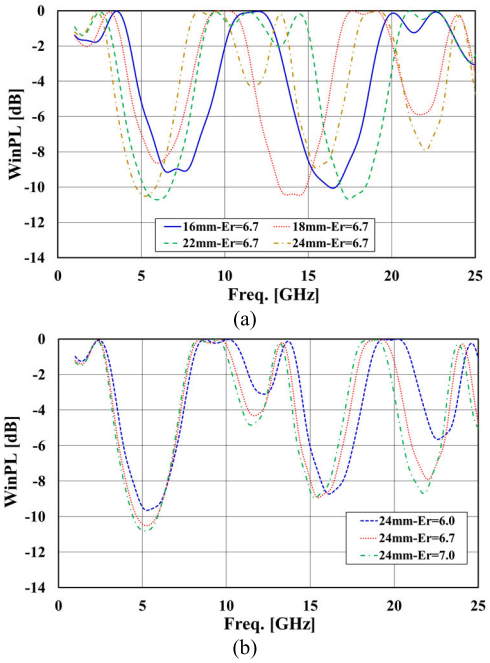

FIGURE 3. WinPL as a function of (a) the structure and (b) permittivity of the glass.

and the observed WinPL changes are more sensitive to the glass construction than to the relative dielectric constant of the glass.

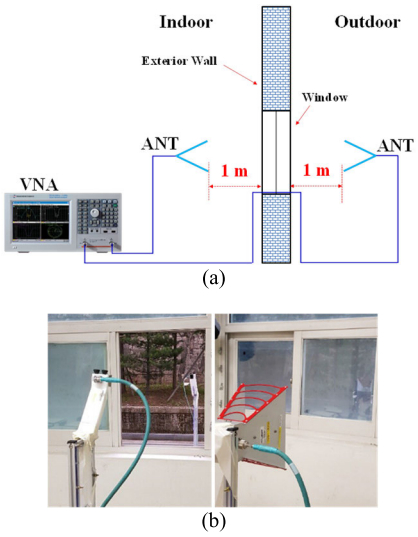

FIGURE 4. Setup (a) for the WinPL measurements and open and closed status of the window in the measurement site using the horn antenna (b).

B. ON-SITE MEASUREMENTS OF WINPL

The measurement setup of WinPL in the building used for the BEL measurements is shown in Figure 4 (a). The antennas were connected via a vector network analyzer (VNA) and were placed inside and outside the outer window at 1.5 m above the ground. These two antennas were connected with a cable through the window frame next to the window to be measured. The distance between the

antenna and wall was 1 m. The measurement frequency ranged from 1 to 25 GHz. Two types of horn antennas were used (ETS-Lindgren 3115 and 3169–09 at 1–18 GHz and 16–25 GHz, respectively) [22]. The 24-mm double-glazed glass window (two 6-mm thick glass panes separated by a 12-mm air gap) was mounted within a metal frame, its size was 126.5 × 113 cm^2, and it consisted of three parts. There are two 56.5 × 56.5 cm^2 frames at the bottom, and a 70 × 113 cm^2 frame is attached above them. Its glass structure was the same as that used in the WinPL simulation. To extract WinPL, the insertion losses (S21 values) were measured when the window was closed and opened, as shown in Figure 4 (b). The difference between these two values can be regarded as WinPL.

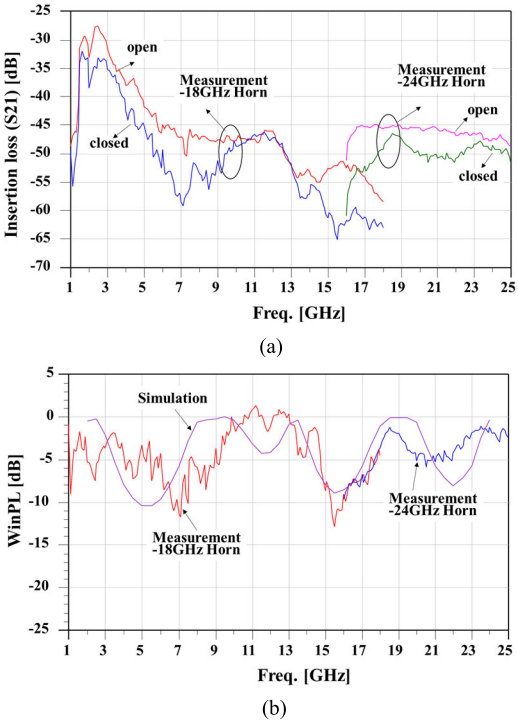

FIGURE 5. Measured insertion losses (a) and WinPL extracted from measurements and simulated (b).

The measured S21 results are presented in Figure 5 (a). It is easy to see that the loss increases in certain frequency bands when the window is closed, but no changes occur in some frequency bands, such as the 1–3, 10–13, and 24–25 GHz bands. In Figure 5 (b), the extracted WinPL results overlap between 16–18 GHz because they were measured with two horn antennas. Positive WinPL results are observed from 11 and 13 GHz. This is because the indoor received power increases due to multiple reflections of radio waves passing through the window without loss. Oscillatory characteristics similar to the simulation result are observed. Small WinPL values are observed at approximately 3, 12, 19, and 24 GHz. On the other hand, high WinPL values over −10 dB are observed at approximately 7 and 15 GHz. Notably, regarding the BEL measurement frequencies at 3.5, 6, 10, 18,

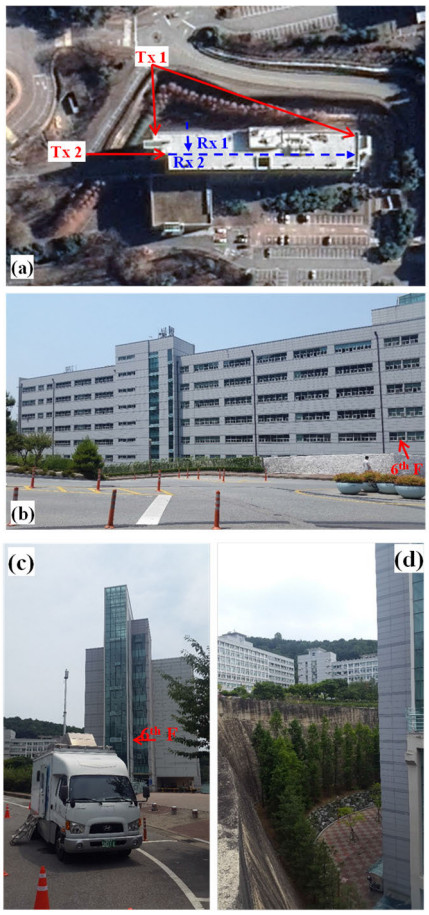

FIGURE 6. Photographs of the building and its surroundings for BEL measurement at Chosun University campus. (a) Tx positions on the road and Rx movement routes in the building, (b) the external façade of the building, (c) Tx 2 antenna on the truck, and (d) a valley between the Tx and the building.

and 24 GHz, the WinPL values are −2.01, −4.20, −0.97, −4.55, and −1.16 dB, respectively. The simulated WinPL result is compared in Figure 5 (b). Despite a direct comparison of the simulation result for a sample of 4 × 4 cm^2 with the on-site measurements of a real glass window with dimensions of 126.5 × 113 cm^2, the two results are different below 10 GHz and relatively consistent above 13 GHz. The reason for the large difference at low frequencies is that the glass window is mounted on three metal frames as shown in Figure 4, and the size of the small frame is smaller than the diameter of the first Fresnel zone, whose value is 36 and 14 cm at 3.5 and 24 GHz, respectively. From simulations and on-site measurements of WinPL for the double glazed glass sample and real windows, respectively, it can be concluded that WinPL has oscillatory characteristics due to the impedance change at a specific frequency as the transmission characteristic of the multilayer dielectric.

III. BUILDING ENTRY LOSS (BEL) CHARACTERISTICS

A. MEASUREMENT ENVIRONMENTS

The BEL measurements conducted in this study were performed in a traditional office building on the Chosun

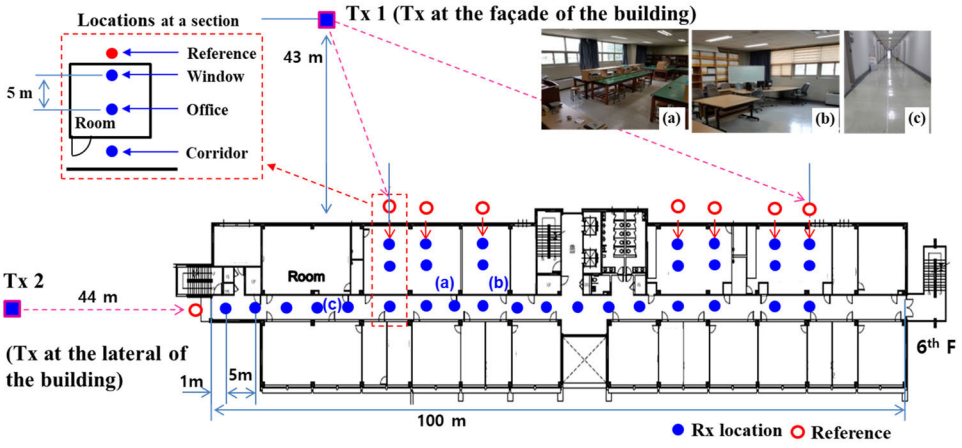

FIGURE 7. BEL measurement scenario [Tx and Rx locations, photos of laboratory (a), seminar room (b), corridor (c) inside the building.

University campus in Gwangju, Korea, as shown in Figure 6. The building is 10 stories tall and features a 35–38-cm thick reinforced concrete shear exterior wall. Each office wall has five double-glazed glass windows without metal coatings. These windows were used to measure WinPL. The building size is 116 m × 31 m. The interior walls of the office building are equipped with plasterboard and foam polyethylene sheets, and the interior wall thickness is approximately 12.5 cm. In this work, two BEL measurement scenarios were performed. Figure 6 (a) shows the locations of the transmitters and the routes of the receivers used in the two BEL measurement scenarios. The transmitter in front of the building is named Transmitter 1 (Tx1), and its antenna is located on the road 43 m away from the building; indoor receiver 1 (Rx1) is located indoors on the 6th floor (6F). Since the road in front of the building is on a 6-story hill, as shown in Figures 6 (b) and (d), the transmitter and receiver antennas are adjusted so that their heights are the same. The transmitter located on the side of the building is named Transmitter 2 (Tx2), and receiver 2 (Rx2) measures the received power only in the corridor of the building. Measurements were conducted at 3.5, 6, 10, 18, and 24 GHz, which are continuous waves (CWs).

B. MEASUREMENT SCENARIOS

Radio waves enter an indoor area, such as an office or corridor, through outdoor walls or windows and propagate to various places through indoor walls, doors, and windows. At this time, radio power is attenuated by multiple reflections and diffraction caused by various clutters. The frequency dependence of these losses is influenced by multiple materials present in indoor environments. It is necessary to analyze the frequency-dependent characteristics of BEL by dividing the indoor propagation path into complex and simple paths.

Therefore, the following two BEL measurement scenarios were used in this work, as shown in Figure 7.

- In the first scenario (complicated route), Tx1 was located on the facade of the building and the received power was measured as Rx1 moved from the edge of a window to the deep corridor inside the building. In this scenario, the radio waves radiated from Tx1 passed through the windows, were reflected multiple times by various clutters in the office, passed through the interior walls and doors, and reached Rx1 in the corridor. The frequency dependence of BEL was analyzed at each location along the complicated route.
- In the second scenario (simple route), Tx2 was placed lateral to the building and the Rx power was measured as Rx2 moved deeper into the corridor. In this scenario, the waves traveled through only the exterior windows, and the structure of these windows was the same as that used in the first scenario and WinPL measurements. Therefore, in this scenario, the frequency dependence of BEL was mainly affected by that of WinPL. In the first scenario, reference power (P_{ref}) values were measured at seven locations using a rod at a distance of 1.6 m from the outer wall, and a receiving antenna was installed at the end of the rod. According to the depth of the building, three measurement locations (window, middle, and corridor) were designated, as shown in the upper right panel of Figure 8, and these were located at distances of 1.0, 5.0, and 10 m from the outer wall, respectively. In the second scenario, the Tx2 antenna was installed on a truck 12 m above the ground and 44 m from the building; this height was the same as the height of the Rx2 antenna in the 6F corridor. P_{ref} was measured at one location, and the method used to measure P_{ref} was the same as that applied in the first scenario. Rx2 measured the power every 5 m along a 100-m corridor. The utilized receiver system, which was mounted on a handcart, was the same in both scenarios, and the antenna was 1.5 m above the floor.

Because Tx1 was not located in the center of the front of the building due to the slope of the road, the incident angles of the radio waves on the left and right sides of the building were 19.03° and 60.12°, respectively, as shown in Figure 7.

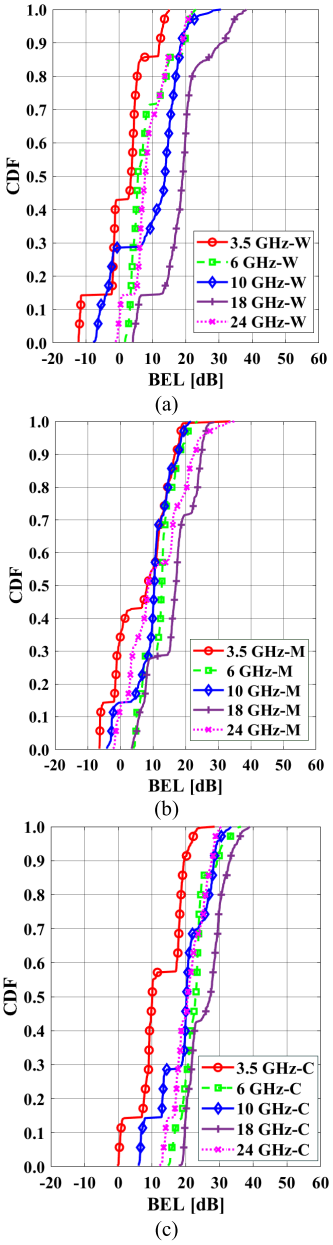

FIGURE 8. Cumulative distribution function (CDF) characteristics of BEL for the first scenario [(a) Window (W), (b) Middle (M), and (c) Corridor (C)].

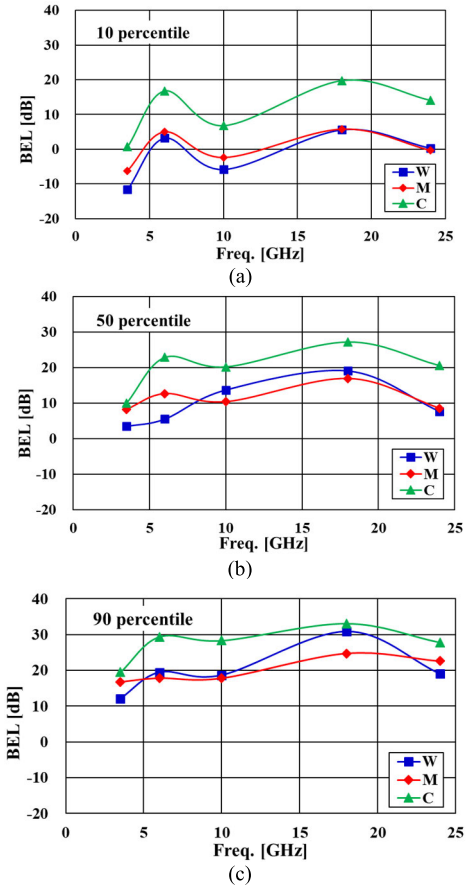

FIGURE 9. Frequency and location dependency of BEL at the (a) 10th, (b) 50th, and (c) 90th percentile levels of CDF.

If Tx1 was located in the center of the front of the building, the incident angle would be 41.09°, and the difference between the incident angles on both sides would be 22.06° and 19.03°. A difference in the BEL value occurs due to a difference in the incident angle, but this difference is expected to be less than 2 dB [19], so its influence on the frequency dependence analysis will not be significant.

C. MEASUREMENT RESULTS

BEL in this study was calculated by using the definition in Recommendation ITU-R P.2040-1 [23] as:

$$P_{indoor} = P_{Tx}+Sys.Para. + FSL+PL_{indoor}+EL$$

$$P_{ref} = P_{Tx}+Sys.Para. + FSL$$

$$BEL = P_{indoor} - P_{ref} = PL_{indoor} + EL \approx PL_{indoor} + WinPL$$

where P_{indoor} is the received power at the indoor locations, P_{Tx} is the transmitted power, Sys. Para. is the summation of all Tx and Rx system parameters, FSL is the outdoor path loss, PL_{indoor} is the indoor path loss, and EL is the excess loss, such as wall or window penetration loss. P_{ref} is the spatial median of the power received outside the illuminated face of a building as the reference power and consists of P_{Tx}, Sys. Para., and FSL. BEL is defined as the difference between P_{indoor} and P_{ref}, and considering that most propagation propagates through windows, BEL is heavily influenced by WinPL.

A cumulative distribution function (CDF) was generated using the calculated BEL values. Figure 8 presents the CDF of the BEL values measured under the first BEL scenario. As in this scenario, Rx is located deeper inside the building than under the first scenario; the BEL values naturally increase from window to middle and the corridor. In the 3.5-, 10-, and 24-GHz cases, when the WinPL values are small, as shown in Figure 6, some negative BEL values are observed in the window and middle locations, but negative BEL values do not occur in the corridor. In general, negative BEL values can be

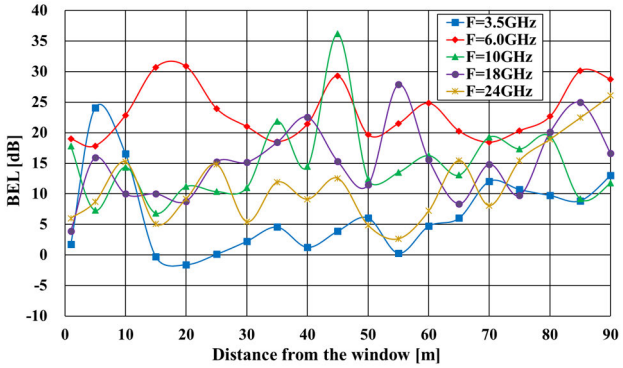

FIGURE 10. BEL characteristics as a function of distance from the window.

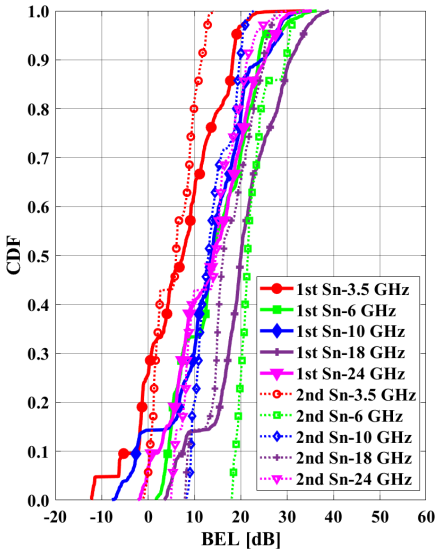

FIGURE 11. Comparison of two BEL scenarios [Sn: the scenario].

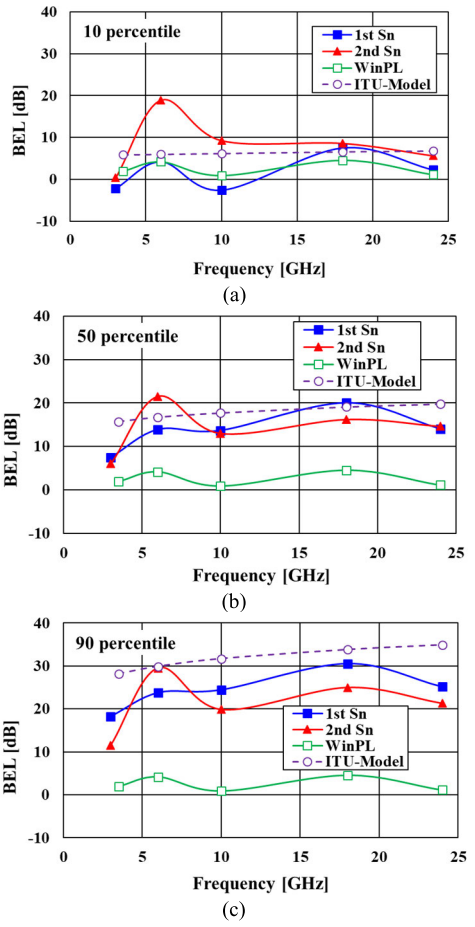

FIGURE 12. BEL at the (a) 10th, (b) 50th, and (c) 90th percentile levels of CDF as a function of frequency and its comparison with WinPL and ITU models.

generated due to multipath reflection [24]. As the Rx moves deeper inside the building, the CDF spread decreases at each location from 50.45 to 41.66 and 39.31 dB because interior walls or doors filter out weak reflected waves in the office, and there is little clutter that causes reflections in the corridor.

The BEL at the 10th, 50th, and 90th percentiles of the CDF is presented in Figure 9 to analyze the frequency dependence of the BEL values. At all measurement locations, the BEL value was higher at 18 GHz than at 24 GHz, and the BEL value was greater at 6 GHz than at 10 or 24 GHz. The frequency dependence of BEL was almost the same as that of WinPL, as shown in Figure 5. Therefore, from the results measured in the first scenario, the following conclusions can be drawn: BEL does not increase linearly with increasing frequency, and in particular, its frequency dependence is maintained even though the measurement point moves deeper from the window to the corridor.

In the second scenario, radio waves that traveled indoors only through the windows on the side of the building were propagated within a 100-m corridor. The propagation route of this scenario was simpler than that of the first scenario. The measured median BEL values are expressed as a function of the distance from the window, as shown in Figure 10. The BEL value fluctuates at 40–60 m at the center of the corridor because stairs, elevators, and bathrooms have complicated the structure. Unlike in the first scenario, negative BEL values are observed at three points and only at 3.5 GHz in the second scenario. It is known that multiple reflections are suppressed due to the relatively simple structure of the corridor. At 6 GHz, the BEL is higher overall than at other frequencies because of the high WinPL value.

The CDF characteristics of the BEL values obtained under the second scenario are compared with those of the first scenario, as shown in Figure 11. Here, in the first scenario, the CDF was generated by summing all BEL values measured at each indoor location. At the 0.5 level of CDF, the BEL values of the two scenarios are similar. However, in the first scenario, the CDF spreads at 3.5, 6, 10, 18 and 24 GHz were 30.77, 19.43, 22.70, 15.06 and 12.57 dB wider than those obtained under the second scenario, respectively, and the CDF difference decreased as the frequency increased. These results indicate that the propagation routes of the first scenario are more complicated than those of the second scenario

and that more multipath reflections are generated under the first scenario.

In Figure 12, the frequency dependences of the BEL are compared with the WinPL values and the values obtained using the ITU BEL model for a traditional building [20] at the 10th, 50th, and 90th percentiles of the CDF. Unlike the outputs of the ITU model, BEL does not increase linearly with increasing frequency, and it has been proven that the frequency dependence follows the characteristics of WinPL regardless of the complexity of the propagation route. In a previous report [19] that compiled BEL data, the same (Chapter 15) or similar (Chapters 22, 24, and 31) characteristics were reported among results measured in the same frequency band as that used in this study. Therefore, it is confirmed that WinPL directly affects the frequency characteristics of BEL. As energy efficiency is emphasized in modern construction, thermally efficient building materials such as double glazed windows are commonly used in traditional buildings. Therefore, the nonlinear frequency dependence of the ITU-R BEL model needs improvement.

IV. CONCLUSION

In this paper, the frequency dependence of WinPL on double-glazed glass was analyzed by simulations and on-site measurements from 3.5 to 24 GHz and compared with the frequency dependence of BEL for traditional office buildings with the same glass windows. In addition, it was compared to that of the ITU-R BEL model. In the WinPL research results using simulations and on-site measurements, it was confirmed that low and high losses are observed at a specific frequency as the transmission characteristic of the multilayer dielectric. In the BEL study for the traditional building with double glazed glass windows, the frequency dependence of the same trend as that of WinPL was observed in the BEL characteristics measured at the front and side of the building using the two measuring scenarios. It has been observed that the frequency dependence of BEL is strongly affected by that of WinPL of windows installed in the building, regardless of complex or simple radio propagation routes. These oscillatory characteristics are different from the linear characteristics of the ITU-R BEL model of traditional buildings, and these differences can lead to inaccurate interference analysis. Some results similar to our study results were presented in ITU-R P. 2346, but these phenomena were not reflected in the ITU-R BEL model. Because of the first version of the model, there are several limitations and revision issues. Therefore, the major contribution of this paper may be an important starting point for future revisions of the ITU BEL model.

REFERENCES

[1] H. Okamoto, K. Kitao, and S. Ichitsubo, "Outdoor-to-indoor propagation loss prediction in 800-MHz to 8-GHz band for an urban area," *IEEE Trans. Veh. Technol.*, vol. 58, no. 3, pp. 1059–1067, Mar. 2009.

[2] E. Semaan, F. Harrysson, A. Furuskar, and H. Asplund, "Outdoor-to-indoor coverage in high frequency bands," in *Proc. IEEE Globecom Workshops (GC Wkshps)*, Austin, TX, USA, Dec. 2014, pp. 393–398.

[3] I. Rodriguez, H. C. Nguyen, N. T. K. Jorgensen, T. B. Sorensen, and P. Mogensen, "Radio propagation into modern buildings: Attenuation measurements in the range from 800 MHz to 18 GHz," in *Proc. IEEE 80th Veh. Technol. Conf. (VTC-Fall)*, Vancouver, BC, Canada, Sep. 2014, pp. 1–5.

[4] R. Rudd, K. Craig, and M. Ganley, "The impact of thermally insulating products on building penetration loss between 100 MHz and 6 GHz," in *Proc. 9th Eur. Conf. Antennas Propag. (EuCAP)*, Lisbon, Portugal, Apr. 2015, pp. 1–3.

[5] V. Kristem, S Sangodoyin, C. U. Bas, M. Käske, J. Lee, C. Schneider, G. Sommerkorn, C. J. Zhang, R. S. Thomä, and A. F. Molisch, "3D MIMO outdoor-to-indoor propagation channel measurement," *IEEE Trans. Wireless Commun.*, vol. 16, no. 7, pp. 4600–4613, Jul. 2017.

[6] I. Rodriguez, H. C. Nguyen, I. Z. Kovács, T. B. Sørensen, and P. Mogensen, "An empirical outdoor-to-indoor path loss model from below 6 GHz to cm-wave frequency bands," *IEEE Antennas Wireless Propag. Lett.*, vol. 16, pp. 1329–1332, 2017.

[7] Y. C. Lee, S.-S. Oh, H. C. Lee, C. W. Byeon, S. W. Park, I.-Y. Lee, J.-H. Lim, J.-I. Lee, and B.-L. Cho, "Measurements of window penetration loss and building entry loss from 3.5 to 24 GHz," in *Proc. 13th Eur. Conf. Antennas Propag. (EuCAP)*, Krakow, Poland, Mar. 2019, pp. 1–4.

[8] Q. Luo, X. Wang, K. Huang, X. Li, and S. Zhang, "A practical evaluation method of building penetration loss at 3.5 GHz for IMT application," in *Proc. 9th Int. Conf. Measuring Technol. Mechatronics Automat. (ICMTMA)*, Changsha, China, Jan. 2017, pp. 150–153.

[9] M. Kowal, S. Kubal, and R. J. Zielinski, "Measuring the shielding effectiveness of large textile materials in an anechoic chamber," in *Proc. Int. Symp. Electromagn. Compat. (EMC EUROPE)*, Rome, Italy, Sep. 2012, pp. 1–4.

[10] M. Yang, A. K. Brown, and S. Stavrou, "Resonant behavior of radio-transmission loss due to periodic building structures," *IEEE Antennas Propag. Mag.*, vol. 53, no. 5, pp. 98–105, Oct. 2011.

[11] M. Pavlik, I. Kolcunova, and L. Lison, "Measuring the shielding effectiveness and reflection of electromagnetic field of building material," in *Proc. 16th Int. Sci. Conf. Electr. Power Eng. (EPE)*, Kouty nad Desnou, Czech Republic, May 2015, pp. 56–59.

[12] A. Karttunen, S. L. H. Nguyen, P. Koivumäki, K. Haneda, T. Hentilä, A. Asp, A. Hujanen, I. Huhtinen, M. Somersalo, S. Horsmanheimo, and J. Aurinsalo, "Window and wall penetration loss on-site measurements with three methods," in *Proc. 12th Eur. Conf. Antennas Propag. (EuCAP)*, London, U.K., 2018, pp. 1–5.

[13] J. R. N. Barbosa, J. C. Rodrigues, S. G. C. Fraiha, H. S. Gomes, and G. P. S. Cavalcante, "An empirical model for propagation loss prediction in indoor mobile communications using Pade approximant," in *IEEE MTT-S Int. Microw. Symp. Dig.*, Brasilia, Brazil, Feb. 2005, pp. 625–628.

[14] S. Stavrou, "Factors influencing outdoor to indoor radio wave propagation," in *Proc. 12th Int. Conf. Antennas Propag. (ICAP)*, Exeter, U.K., 2003, pp. 581–585.

[15] K. Sayidmarie, A. H. Aboud, and M. S. Salim, "Estimation of wall penetration loss for indoor WLAN systems," in *Proc. 6th Int. Conf. Sci. Electron., Technol. Inf. Telecommun. (SETIT)*, Sousse, Tunisia, Mar. 2012, pp. 675–679.

[16] Y. Du, C. Cao, X. Zou, J. He, H. Yan, G. Wang, and D. Steer, "Measurement and modeling of penetration loss in the range from 2 GHz to 74 GHz," in *Proc. IEEE Globecom Workshops (GC Wkshps)*, Washington, DC, USA, Dec. 2016, pp. 1–6.

[17] L. Yishan, Z. Feng, S. Jinglu, C. Kai, G. Bolun, and W. Yong, "Analysis and measurment of wall penetration loss as a function of incident angle," in *Proc. Int. Workshop Electromagnetics, Appl. Student Innov. Competition*, London, U.K., May 2017, pp. 124–125.

[18] R. Rudd, K. Craig, M. Ganley, and R. Hartless. (2014). *Building Materials and Propagation*. Final Report, Offcom. [Online]. Available: https://www.ofcom.org.uk

[19] *Compilation of Measurement Data Relating to Building Entry Loss*, document ITU-R P.2346-3, 2017.

[20] *Prediction of Building Entry Loss*, document ITU-R P.2109-0, Recommendation, 2017.

[21] *CST Microwave Studio Suite*. [Online]. Available: https://www.cst.com/

[22] *Double-Ridged Waveguide Horn Antennas*. [Online]. Available: http://www.ets-lindgren.com/get-manuals/3112(1).pdf

[23] *Effects of Building Materials and Structures on Radio Wave Propagation Above About 100 MHz*, document ITU-R P.2040-1, Recommendation, 2015.

YOUNG CHUL LEE received the B.S. and M.S. degrees in electronic engineering from Yeungnam University, Gyeongsan, South Korea, in 1995 and 1997, respectively, and the Ph.D. degree in electronic engineering from Information and Communications University (ICU; merged with Korea Advanced Institute of Science and Technology (KAIST), in 2009), Daejeon, South Korea, in 2005. From 1997 to 2000, he was with the Research and Development Division, LG Semicon Inc., Cheongju, South Korea, where he was involved in the development of MOSFET devices for DRAM applications. Since 2005, he has been with Mokpo National Maritime University, Mokpo, South Korea, where he is currently a Full Professor with the Division of Marine Mechatronics. From 2008 to 2013, he participated in 60 GHz and E-band wireless system research as a Technical Consultant at Telecom Malaysia Research and Development (TMRND), Malaysia. Since 2016, he has been interested in radio wave propagation for ITU-R propagation model applications and he is developing wireless power transmission and energy harvesting technology for propulsion shaft applications. His research interests include millimeter-wave circuits and systems, 3D integration of RF circuits using LTCC-based system-in-package (SiP) technology, and reconfigurable RF circuits.

SOON-SOO OH was born in Yeosu, Republic of Korea, in 1972. He received the B.S. and M.S. degrees in electronics engineering from Inha University, Incheon, South Korea, in 1998 and 2000, respectively, and the Ph.D. degree in radio sciences and engineering from Korea University, Seoul, South Korea. From May 2005 to August 2013, he was a Senior Member of Engineering Staff with the Electronics and Telecommunications Research Institute (ETRI). He has been an Assistant Professor, since September 2013, and an Associate Professor, since September 2017, with the Department of Electronics Engineering, Chosun University, Gwangju, South Korea. His research interests include the analysis/design of array antennas, electromagnetic field measurements, and radio wave propagation.

CHUL WOO BYEON (Member, IEEE) received the Ph.D. degree in electronic engineering from KAIST, Deajeon, South Korea, in 2013.

His Ph.D. research concerned low-power millimeter-wave/RF integrated circuit, antenna, and package design. Since 2013, he has been a Postdoctoral Researcher with the Department of Electrical and Computer Engineering, UCSD. From 2014 to August 2015, he was a Senior Engineer with Samsung DMC R&D Center, Suwon, South Korea. In September 2015, he joined the Department of Electronic Engineering, Wonkwang University, Iksan, South Korea, where he is currently an Associate Professor. His research interests include CMOS/SiGe RF/millimeter-wave/THz integrated circuits, antenna, package, and system design for wireless communications.

KHAIRUNNISA AZIDING received the Bachelor of Communication Engineering degree (Hons.) from International Islamic University Malaysia (IIUM), Gombak, Malaysia, in 2019. She is currently pursuing the Master of Engineering degree with the Department of Electronics, Communication and Computer Engineering with a focus on radio wave propagation as her major research. She has been a Graduate Research Assistant with Mokpo National Maritime University, Mokpo, South Korea, since August 2019.

BYUNG-LOK CHO received the B.S., M.S., and Ph.D. degrees in electronics engineering from Sungkyunkwan University, Suwon, South Korea, in 1987, 1990, and 1994, respectively. From 1987 to 1988, he was a Researcher with Samsung Electronics, Inc. From 2001 to 2002, he was with the University of California at Davis, Davis, USA, as a Visiting Researcher. He is currently a Full Processor with Sunchon National University, Suncheon, South Korea. His research interests include the analysis/design of ultra-wideband and the Internet of Things (IoT).